Collision-Induced Optical Phase

P. J. Laverty, K. D. Stokes, and J. E. Thomas
Physics Department, Duke University, Durham, North Carolina 27706
(Received 8 August 1988)

New techniques are demonstrated which measure, for the first time, collision-induced *phase* in macroscopic optical coherence. The shape of the phase versus time-delay curves obtained from the data yields the first information on *imaginary* velocity-changing collision kernels for optical radiators.

PACS numbers: 34.40.+n, 42.50.Md

Since the early 1970s, it has been appreciated that a complete description of velocity-changing collisions for optical radiators (optical coherence) in vapors requires a quantum-mechanical treatment for both the internal and center-of-mass degrees of freedom.[1-3] This is due to the fact that an optical radiator consists of a superposition of ground and excited electronic states, each of which is shifted and deflected differently in a collision with a perturber. Hence, a well-defined classical collision trajectory may not exist. In collision experiments which study the motion of optical radiators, only the oscillating part of the atomic charge distribution is observed in the measurement. The differential scattering cross section for the optical radiator is then determined by the overlap of the quantum-mechanical scattering amplitudes for the superposed states. When the collision potentials for the superposed states are not identical the differential scattering cross section will not be real. Physically, this is due to the phase change acquired by the optical radiator during a collision. As a consequence, the corresponding collision-induced velocity-change distribution (i.e., the velocity-changing kernel) and the total collision cross sections will have both a *real* and an *imaginary* component.[4]

Considerable information on the real part of the velocity-changing kernel for infrared and optical radiators has been obtained by measuring the time-dependent decay of the intensity of two-pulse photon echoes. The long measurement time scales obtainable with photon echo techniques yield correspondingly high velocity resolution. Radiator destruction and velocity-changing cross sections, and average velocity changes per collision, have been measured by this technique for infrared[5,6] and optical radiators.[7,8] It has been demonstrated that the real part of the velocity-changing kernel for an optical radiator is principally diffractive, the measured velocity changes exhibiting perturber mass and total cross-section scaling and magnitude characteristic of diffraction.[8]

Imaginary kernels, by contrast, appear to be relatively unexplored, although they are a unique feature of the scattering of superpositions of dissimilar states. Unlike the real kernel, for which long-range interactions with small phase shifts make important contributions, the imaginary kernel requires for its existence a nonzero phase shift. It is therefore particularly well suited to investigating large-phase-shift effects such as "trajectory separation,"[4] which arises when the classical paths for the superposed states do not coincide. Prior to the work presented here, only indirect information on imaginary kernels had been obtained, from the nonlinear pressure dependence of the line shift measured for infrared radiators.[9]

In this Letter, we report the measurement of time-dependent collision-induced *phase* for macroscopic optical coherence in Yb vapor.[10] The measured phase versus time curves are applied to study *imaginary* collision kernels and total cross sections for radiator–rare-gas scattering. The imaginary part of the total collision rate is found to be much smaller than the usual pressure shift. The width of the imaginary part of the velocity-changing kernel appears to be much larger than that of the real part, suggesting that classical velocity changes may make a major contribution to the imaginary kernel. This is in contrast to earlier work on the real part of the velocity-changing kernel, where it appears that optical radiator scattering is dominated by diffractive scattering.[7,8]

In the experiments, Fig. 1, a Ramsey fringe is induced in the population velocity distribution of a two-level atomic vapor (^{174}Yb) by exciting the $^1S_0 \rightarrow {}^3P_1$ transition at 556 nm using two optical pulses (~ 10 mW/mm^2) separated by a time delay, T. The pulses are generated by acousto-optic modulation of stable cw dye laser radiation.[8] At a time just after $2T$ (see below) relative to the first input pulse, the absorption, α, of a weak counterpropagating cw probe wave (~ 0.2 μW) originating from the same laser is measured as a function of laser frequency detuning, Δ. Because of the population fringe, the probe absorption signal contains a fringelike component, which for short pulses takes the form[11]

$$\alpha(\Delta) = A(\Delta)\cos[2\Delta T + \varphi(2T)], \quad (1)$$

where $\Delta = \omega - \omega_0 + \omega_{AO}/2$ and ω is the laser frequency, ω_0 is the atomic resonance frequency, and ω_{AO} is the frequency shift of the acousto-optic modulator. The collision-induced *phase* at time $2T$, $\varphi(2T)$, is determined by comparing signals from two cells at different perturber pressures, Fig. 2, as a function of Δ.

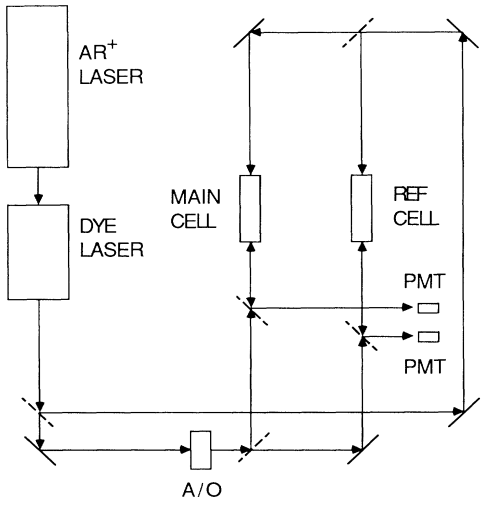

FIG. 1. Experimental scheme.

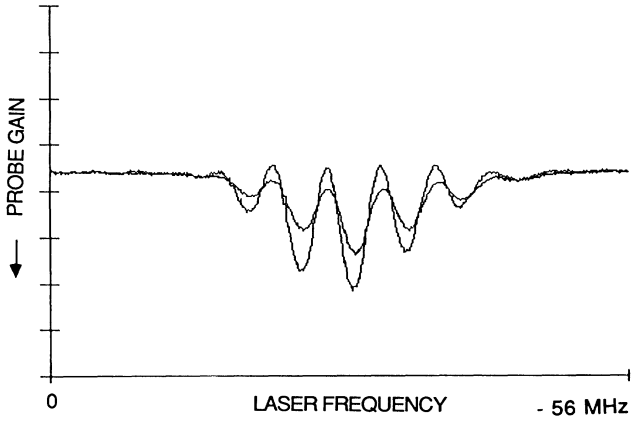

FIG. 2. Probe absorption vs laser frequency. The larger (smaller) signal corresponds to the reference (main) cell. Laser frequency increases to the left.

Probe absorption fringe signals are predicted theoretically[12] and found experimentally to peak at a time $2T$ relative to the first input pulse. (This arises from the cosinusoidal distribution of Doppler-shifted frequencies radiated by the sample.) Further, the phase $\varphi(2T)$ does not change after the time $2T$, when the probe-induced polarization comes into equilibrium and tracks the population inversion. It is for this reason that signal measurements are made just after the time $2T$.

The phase $\varphi(2T)$ is determined for a number of time delays T in order to obtain a phase versus time-delay curve, Fig. 3. As discussed below, $\varphi(2T)$ is a nonlinear function of T from which the imaginary part of the velocity-changing kernel can be determined by Fourier transformation.

Physically, Eq. (1) can be understood as follows. Just after the first input pulse, a macroscopic polarization is created in the medium, where each atom radiates at a frequency ω_0 in its rest frame. The power absorbed by a given group of atoms from the second pulse depends on the relative phase of the field and the polarization at time T. For atoms moving at speed v along the pulse propagation direction, the phase is just $\phi=(\omega+\omega_{AO}-kv-\omega_0)T$ in the absence of collisions, where k is the optical wave vector, $2\pi/\lambda$. Hence, a population inversion with a fringelike velocity dependence $\propto\cos\phi$ is created in the medium after the second pulse, due to the Doppler shift kv. The absorption of a weak counterpropagating probe wave depends on the population inversion of a selected velocity group v such that $\omega+kv=\omega_0$. Solving for the selected v and inserting in the time-dependent phase ϕ yields $\phi=2\Delta T$ and fringelike absorption as in Eq. (1).

In the presence of collisions, the macroscopic polarization is altered during the period T between the first and the second pulses, and during the probe-induced polarization buildup time T between the second pulse and the signal measurement time $2T$. Both destruction and velocity changes occur, causing nonexponential decay of the amplitude of the fringelike absorption signal, analogous to that measured in echo experiments.[4,8] In addition, the phase of the absorption signal is shifted according to

$$\varphi(2T)=-2\,\mathrm{Im}\int_0^T\Gamma_{ba}(t)dt\,. \tag{2}$$

The time-dependent decay rate is

$$\Gamma_{ba}(t)=\gamma_{\mathrm{tot}}-\int_{-\infty}^{\infty}d(\Delta v)W_{ba}(\Delta v)\cos(k\,\Delta v\,t)\,. \tag{3}$$

This result is of the same form and uses the same approximations as in the analysis of echo experiments,[4]

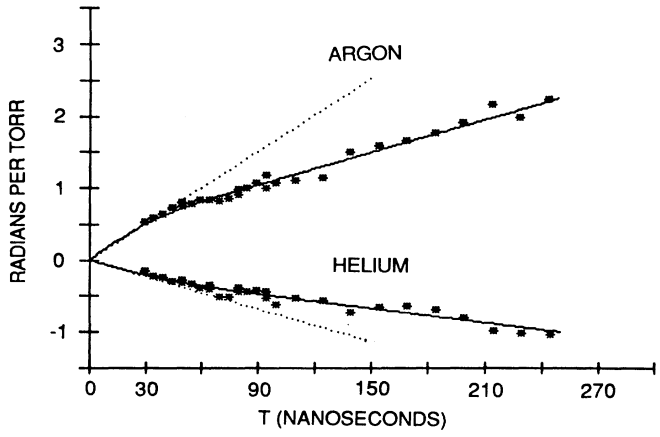

FIG. 3. Collision-induced phase $\varphi(2T)$ vs time delay T. Dotted lines show the short-time fit $\varphi(2T)=-2\delta_s T$ for the pressure shifts obtained from the Lamb-dip data.

where the real part of the integral appearing in Eq. (2) is measured. Equation (3) shows that the imaginary part of the one-dimensional collision kernel, $W_{ba}(\Delta v)$, is related by Fourier transformation to the phase $\varphi(2T)$. It is assumed in writing Eq. (3) that the one-dimensional kernel is a function only of the velocity change, Δv, along the laser pulse propagation direction. This approximation is valid for excitation near the center of the Doppler profile for the small-angle velocity changes which the radiator survives, provided that the initial and final radiator velocities are small compared to the perturber thermal speed.[13]

The factor of 2 in the time-dependent phase of Eq. (2) arises from the evolution of the macroscopic coherence in two ways. Between the two input pulses separated by a delay T, collisions shift the phase of the optical coherence, causing a shift of the population fringe. In addition, during the time interval T between the second input pulse and the measurement time $2T$ (as discussed above), collisions shift the phase of the probe-induced polarization relative to the probe field. The net phase of the probe absorption fringe is just the sum of these two identical phase shifts. At small time delays T, the rate $\mathrm{Im}\Gamma_{ba}(t)$ reduces to the usual line shift, δ_s, independently of the details of the kernel shape.[4] In this case $\varphi(2T) = -2\delta_s T$, exactly the result one obtains by shifting the resonance frequency ω_0 by δ_s in the time-dependent phase ϕ above. In general, for a given pulse delay, only velocity changes smaller than $\sim\lambda/T$ can cause phase shifts without degrading the amplitude of the fringelike absorption signal. Hence, the pulse separation controls the velocity resolution, resulting in the nonlinear dependence of the phase on T. As $T\rightarrow\infty$, the slope of the phase versus time-delay curve is $-2\,\mathrm{Im}\gamma_{\mathrm{tot}}$, where $\mathrm{Im}\gamma_{\mathrm{tot}}$ is the imaginary part of the total collision rate. This is *independent* of the details of the kernel shape.[4]

To measure the phase $\varphi(2T)$ for a fixed input-pulse separation T, fringelike absorption traces are recorded as functions of laser frequency simultaneously in two absorption cells, a reference cell with no perturber, and a main cell at a perturber pressure between 0 and 300 mTorr of rare gas. The phase $\varphi(2T)$ is extracted by fast Fourier transformation of the two traces. From the amplitudes of the sine and cosine transforms at the fringe frequency, the phase of the traces at the origin of the scan is readily found. The *relative* phase between the main- and reference-cell fringes is quite accurately determined, typically within 0.01 rad. By plotting the relative phase of the absorption fringes as a function of perturber pressure, one obtains a straight line where the slope is the collision-induced phase per Torr of perturber gas, $\varphi(2T)$ for pulse separation T.

In order to map out the collision-induced phase versus time curve systematically, a computer-controlled delay generator (SRS DG535) is used to control pulse timing for a home-built pulse-duration generator, the output of which is sent to the acousto-optic modulator. In addition, the delay generator is used to control the gate timing for two boxcar averagers which sample the probe absorption signals at time $2T$. Fringelike absorption signals are obtained by scanning the laser frequency through $\sim$56 MHz (84 MHz for the shortest time delays). Frequency scans are divided into 512 points at each of which the boxcar averages 100 samples. At a repetition rate of 17 kHz, a typical scan takes 2.5 s. The absolute laser frequency is not stabilized, since the relative phase between the signal and reference cells is all that is required. However, to avoid drift of the signals with respect to the scan range, the computer is programmed to shift the ramp start frequency to maintain centering. Further, analog-to-digital gains are adjusted automatically and the cell temperatures are servo stabilized at $\sim$320°C. In this way many hundreds of data curves are obtained in just a few minutes. In a typical run, five frequency scans at each of twenty T values are recorded for each of six main-cell pressures.

Figure 3 shows phase versus time curves for argon and helium perturbers. Data taken for time delays between 60 and 245 ns for argon and helium fall on a nearly straight line with nonzero y intercept and a slope which determines $\mathrm{Im}\gamma_{\mathrm{tot}}$ independently of the details of the kernel shape (see Table I). Since the *collision-induced* phase must cross the origin at zero time delay T, it is evident that the data must curve, as expected when velocity-changing collisions are present.

Time resolution in the experiments was limited by the pump pulse duration of 12 ns so that the detailed shape of the phase versus time curve could not be obtained. However, from the short-time data, the pressure shifts are obtained (Table I), using $\varphi(2T) = -2\delta_s T$ as discussed above. Pressure shifts were also measured independently, using a Lamb-dip technique to obtain Doppler-free resonances in the reference and signal cells. Fifty scans each were taken with the reference cell at zero perturber pressure, and the signal cell at 0-, 500-, and 1000-m Torr perturber pressure. The pressure shifts of the broad lines yield for argon perturbers, $\delta_s = -1.34 \pm 0.13$ MHz/Torr, and for helium, $+0.60 \pm 0.06$ MHz/Torr, in excellent agreement with the shifts obtained from the phase versus time data (see dotted lines Fig. 3).

An estimate of the width of imaginary collision kernel was obtained by assuming a Gaussian velocity-change distribution of $1/e$ width δv and velocity-change integral

TABLE I. Imaginary-kernel collision parameters.

Perturber	δ_s (MHz/Torr)	$\mathrm{Im}\gamma_{\mathrm{tot}}$ (MHz/Torr)	δv (cm/s)
He	$+0.58 \pm 0.06$	$+0.26^{+0.04}_{-0.04}$	350^{+175}_{-120}
Ar	-1.50 ± 0.15	$-0.60^{+0.04}_{-0.05}$	479^{+122}_{-76}

$\mathrm{Im}\gamma_v$, the imaginary part of the velocity-changing rate. This is determined from the above measurements, independently of the kernel shape, as $\mathrm{Im}\gamma_v = \mathrm{Im}\gamma_{\mathrm{tot}} - \delta_s$.[4] Using Eqs. (2) and (3), the width of the kernel is determined by requiring that the theoretical phase (solid curve, Fig. 3) fit the phase versus time data using the kernel width as the only free parameter. The y intercept of the long-time delay asymptote is most sensitive to the kernel width.

The results of the measurements, Table I, show that the imaginary part of the total collision rate is smaller than the line shift, in contrast to the real part, which is larger than the broadening rate.[8] This is reasonable, since the imaginary part of the total collision rate is the line shift excluding the contribution of the velocity-changing kernel which destroys the fringe in the population inversion when T is large. Hence, the largest velocity changes which cause the largest collision-induced phase shifts do not contribute.

A most important feature of this work is that the width of the imaginary kernel appears to be much larger than that of the real kernel, where a Gaussian distribution also was assumed.[8] For argon perturbers, the width falls in the classical region, about 8 times the diffractive width observed for the real kernel.[8] This probably is due to the fact that the imaginary kernel does not exist unless the collision-induced phase of the superposed states is nonzero. For long-range collisions, the phase shifts are small and the kernel is predominantly real. In addition, the width for helium perturbers falls below that for argon. By contrast, for the real kernel, the width for helium perturbers is twice that obtained for argon, as expected for diffractive collisions.[8]

In conclusion, we have demonstrated a new technique for measuring collision-induced optical phase in vapors. This technique has been applied to study imaginary collision kernels for optical radiators by exploiting the Fourier-transform relationship between the shape of the measured phase versus time curve and the kernel. At present, the measurements are limited by the rise time of the optical pump pulses employed in the experiments, a deficiency which will be remedied in future work. However, the results of the experiments suggest that Yb optical radiators survive much larger velocity changes than previously measured[8] or expected on the basis of trajectory-separation arguments for dissimilar states.[4] With shorter input pulses, it will be possible to obtain complete imaginary kernels by Fourier-transform inversion as achieved previously for real kernels.[14,15] Finally, time-dependent optical phase measurements should be generally applicable in vapors and condensed-matter systems with inhomogeneous broadening, where phase measurement may provide new information.

It is a pleasure to acknowledge stimulating discussions with S. Cameron, S. Zilio, and M. S. Feld. This work is supported by the U.S. National Science Foundation through Grant No. PHY-8703664.

[1]E. W. Smith, J. Cooper, W. R. Chappell, and T. Dillon, J. Quant. Spectrosc. Radiat. Transfer **11**, 1547 (1971); **11**, 1567 (1971).

[2]P. R. Berman, Phys. Rev. A **5**, 927 (1972).

[3]See V. A. Alekseev, T. L. Andreeva, and I. I. Sobelman, Zh. Eksp. Teor. Fiz. **62**, 614 (1972) [Sov. Phys. JETP **35**, 325 (1972)], and references therein.

[4]For a recent review, see P. R. Berman, T. W. Mossberg, and S. R. Hartmann, Phys. Rev. A **25**, 2550 (1982).

[5]J. Schmidt, P. R. Berman, and R. G. Brewer, Phys. Rev. Lett. **31**, 1103 (1973).

[6]See R. L. Shoemaker, Annu. Rev. Phys. Chem. **30**, 239 (1979), and references therein.

[7]R. Kachru, T. J. Chen, S. R. Hartmann, T. W. Mossberg, and P. R. Berman, Phys. Rev. Lett. **47**, 902 (1981).

[8]R. A. Forber, L. Spinelli, J. E. Thomas, and M. S. Feld, Phys. Rev. Lett. **50**, 331 (1983).

[9]See, for example, S. N. Bagaev, E. V. Baklanov, and V. P. Chebotaev, Pis'ma Zh. Eksp. Teor. Fiz. **16**, 344 (1972) [JETP Lett. **16**, 243 (1972)].

[10]J. E. Thomas, P. Laverty, and K. Stokes, Bull. Am. Phys. Soc. **33**, 1011 (1988).

[11]For finite-duration pulses, a simple amplitude calculation gives the exact result, but the conclusions obtained here based on intuitive arguments are unaltered.

[12]J. E. Thomas *et al.* (to be published).

[13]For a discussion of this point, see Ref. 4, and J. M. Liang, L. A. Spinelli, R. W. Quinn, R. R. Dasari, M. S. Feld, and J. E. Thomas, Phys. Rev. Lett. **55**, 2684 (1985); J. E. Thomas, A. P. Ghosh, and M. A. Atilli, Phys. Rev. A **33**, 3029 (1986).

[14]C. D. Nabors, B.S. thesis, Massachusetts Institute of Technology, 1984 (unpublished).

[15]A. G. Yodh, T. W. Mossberg, and J. E. Thomas, Phys. Rev. A **34**, 5150 (1986).